# CYCLIC BEHAVIOR OF COLD-FORMED STEEL FRAMES WITH STRAP BRACING

Y. Hosseinzadeh, A. Moslehifar and H. Ahmadi[*]
Faculty of Civil Engineering, University of Tabriz, Tabriz 5166616471, Iran

## ABSTRACT

In the present research, inelastic behavior of cold-formed steel frames with strap bracing was studied under cycling loading using finite element (FE) method. All of frame members including tracks, studs, and braces were modeled using two dimensional shell elements. The screw connections of braces to studs were simulated using connector elements. The shear and axial strength of screws were determined considering the screw pull-out and hard contact of braces to studs. The failure mechanism and resultant base shear were compared with the experimental measurements. The results showed a good agreement between developed FE model and experimental data. The shear and tensile forces of screws at different stages of loading, as well as the behavior in elastic and inelastic regions, were evaluated using the developed model. It was concluded that the buckling and yielding of braces are the most effective factors on the cyclic behavior of cold-formed steel frames; and that cyclic behavior of cold-formed steel frames with strap bracing can be accurately determined using the proposed FE model.

## 1. INTRODUCTION

The use of cold-formed steel (CFS) in the main framing elements of a structure is becoming more popular for the construction of low- to mid-rise buildings, including areas with a high seismic hazard. However, many of the design codes currently have no seismic provisions for cold-formed steel construction. The North American standard for CFS framed lateral systems [1] contains seismic design, material and detailing information. This standard was recently made available by the American Iron and Steel Institute (AISI) to address, in part, the lack of relevant code provisions in Canada. The 2007 version of AISI S213 contains requirements for the brace material and the use of capacity design principles [2]. In recent

---

[*]E-mail address of the corresponding author: h-ahmadi@tabrizu.ac.ir (H. Ahmadi)

years, there have been many studies on CFS wall studs with diagonal straps. However, as far as the authors are aware, research on the seismic performance of CFS walls has been rather limited.

Adham et al. [3] evaluated the lateral load versus deflection behaviour of six 2.44×2.44 m cold-formed steel planar frames sheathed with steel straps and gypsum. Results of this study showed that stud buckling will lead to a severe degradation in the shear load that can be applied to the wall. However, when this mode is properly addressed in design, strap braced systems are effective in dissipating energy under reversed cyclic loading.

Al-Kharat and Rogers [4, 5] showed that if capacity design principles are not adhered to it is possible for the wall to fail in a non-ductile mode rather than maintaining its resistance in the inelastic range by means of brace yielding. Tension fracture of the anchor rods, punching shear or compression failure of the tracks, compression failure of the chord studs, net section fracture of the braces or brace connection failure may occur instead, resulting in both a loss of strength and a decrease in ductility.

Kim et al. [6] performed a shaking table test on a full-scale two-storey one-bay CFS shear panel structure. The results showed that during the large amplitude tests, the X-strap bracing showed very ductile, but highly pinched, hysteretic behavior. The results of this study can be considered conservative because the effect of non-structural gypsum board cladding was not considered in the test.

A study by Filiatrault and Tremblay et al. [7] on the design of tension-only concentrically braced frames (TOCBF) for seismic impact loading used hot-rolled steel as the brace material. Shaking table test results from a two storey TOCBF structure and subsequent high strain rate tests on coupon samples revealed that an amplification factor of 1.15, applied to the yield tensile resistance, is appropriate for use in capacity based design.

Hatami et al. [8] conducted laboratory tests on 2.4m×2.4m wall specimens using different strap connection locations and configurations. It was found that when the straps were attached to the tracks away from the corners wall performance was poor due to track bending and early buckling of studs located adjacent to brace ends.

For the studies on the cyclic behavior of other types of framing systems and bracings, the reader is referred for example to Husem et al. [9], Dalalbashi Esfahahi et al. [10], and Sharbatdar et al. [11], among others.

Most of studies on cold-formed frames were experimental and consequently expensive. Hence, it is necessary to develop theoretical methods such as a finite element (FE) procedure to evaluate the behavior of such systems. According to the knowledge of the authors, there is no report available in the literature on the use of complex finite element models to predict the behavior of the CFS systems.

In the present research work, an FE model was developed to investigate the cyclic behavior of cold-formed steel frames with steel strap braces. The FE model was developed using ABAQUS [12]. The nonlinear behavior of steel material under the cyclic loading and the effect of geometric nonlinearity were included for the development of the model. The S4R shell elements were used for the mesh generation. A method for simulating the behavior of self-drilling screws was used for the connections of strap braces and studs with connector elements. In this method, it is possible to simulate the rigid behavior of screws with regard to shear and axial ruptures, and also screw-head pull-out. Hard contact between

braces and studs, cyclic loading, and nonlinear dynamic analysis were other features of the FE model. This model was confirmed by experimental data presented in Ref. [2]. Following objectives were considered in the present paper: The investigation of various regions of hysteresis loops, identification of failure mechanisms of the frame, and determination of internal forces in screws and base shears. The developed FE model was used to study the seismic behavior of cold-formed steel frames with strap bracing.

## 2. FE MODELING, ANALYSIS, AND VERIFICATION

### 2.1 Details of FE modeling

A three dimensional FE model was created by the use of S4R reduced-integration shell elements in ABAQUS V6.10-1 [12]. The formulation of this type of element is suitable for large strains. Thick shell behavior was employed in the element formulation. The number of integration points along the thickness of elements was increased to nine, in order to simulate severe bucking in braces and to increase the accuracy of the model. The convergence test was done on all members to determine the appropriate sizes for elements. Linear kinematic hardening plasticity model was used to take into account the Boshinger effect.

Required experimental data on cold-framed steel frames with various bay length-to-frame height ratios under cyclic loading were obtained from Ref. [2]. In the present work, a light frame (14 A-C) with equal ratio of bay length to frame height was selected for modeling. Details of frame members' dimensions together with the material properties are presented in Table 1. The schematic depiction of the light frame (14 A-C) is presented in Fig. 1. This figure shows dimensions of the frame, support conditions of tested specimen, and actuator position. In this specimen, tracks and studs were single C-shaped cross sections and chord studs were double back-to-back C-shaped cross sections with bolted connections. Studs were screw connected to the braces with No. 8×1/2 in self drilling wafer head screws. The studs and braces at corners of frame were connected by welding. S/HD10S Simpson hold-downs were used to increase the rigidity of the frame at the corners [2].

Table 1: Characteristics of test specimens for strap-braced walls

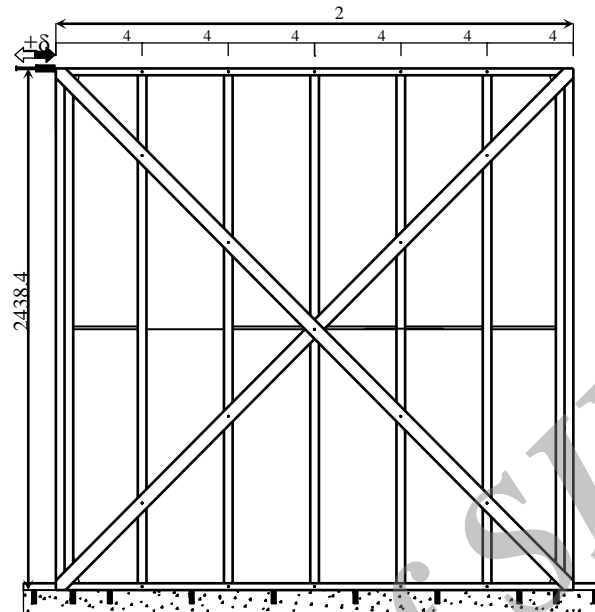| ID: 14 A-C | Nominal dimensions | | Material properties | | | |
|---|---|---|---|---|---|---|
| | Dimensions (mm) | Thickness (mm) | $E$ (GPa) | $F_y$ (MPa) | $F_u$ (MPa) | $\varepsilon_u$ (%) |
| Strap bracing | 63.5 | 1.09 | | 307 | 375 | 31.6 |
| Studs | 92×41×12.7 | 1.09 | 210 | 325 | 382 | 28.8 |
| Tracks | 92×31.8 | 1.09 | | 296 | 366 | 32.5 |

Figure 1. Schematic depiction of light wall (14 A-C) components (unit: mm)

A rigid base was generated in the FE model and lower track at the anchor rod location was fixed via fastener constraint with definite effective radius. To simplify the model, screw connection of studs to tracks and back-to-back connection of chord studs were made completely rigid using Tie constraint. Rigid behavior of braces' screw connection to studs, the effect of screw diameter, their axial and shear strength, and pull-out strength of screws were considered in modeling. For this purpose, holes were created with a diameter equal to the diameter of screws in both brace and studs. Nodes around these holes were connected, using rigid beam elements, to the reference points at the top of brace and the bottom of studs' plate. Afterwards, these two reference points were connected by Radial-Thrust connector element. Axial and radial stiffness of this type of element were considered as rigid in order to simulate the real behavior of screws. Shear and pull-out failures were also considered by applying ultimate axial and shear strength. Axial strength for pull-out failure and shear strength were 1.47 kN and 2.35 kN based on screw type, respectively [13]. Details of screw modeling are shown in Fig. 2. The contact with the possibility of plate separation between braces and studs with the friction coefficient of 0.3 was defined during the modeling.

*2.2 Nonlinear analysis*
The analysis of FE model was performed by DYNAMIC/EXPLICIT option. The model loading was controlled displacement at the level of the roof. The time history of loading during the experiment has been given in Fig. 3. This time history was introduced to the software by smooth curves to eliminate the effects of impact and static loads.

In DYNAMIC/EXPLICIT type of analysis, the application of very small elements leads to the increase of computational time. To resolve this problem, the mass of small elements was increased 30 percent using mass scale option. The stability time of these elements

approaches to the average stability time of other elements by applying this virtual mass. The accuracy of analysis was set to double mode to reduce data rounding errors corresponding to large number of analysis increments (about 50 millions).
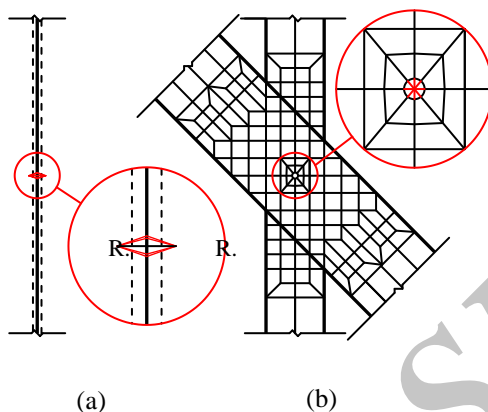


(a)                              (b)

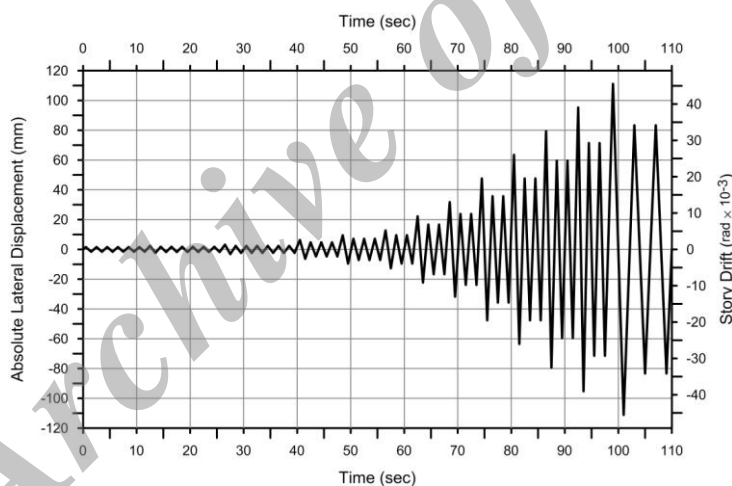Figure 2. Details of FE modeling of screws: (a) lateral view, (b) front view



Figure 3. Time history of loading

### 2.3 Model verification

Results of FE analysis for deformed shape of cold-formed frame and the hysteresis curve of base shear-lateral displacement are presented in Figs. 4 and 5, respectively. Numerical results of FE analysis compared with those of test data are given in Table 2. It can be seen that experimental and numerical hysteresis curves of base shear-lateral displacement have good agreement. Maximum errors for elastic lateral stiffness and ultimate base shear were 3.04% and 7.65%, respectively. Failure mode in numerical model was the buckling in strap braces that is consistent with failure mode reported during the experiment. No shear failure or pull-out was observed in screws [2].
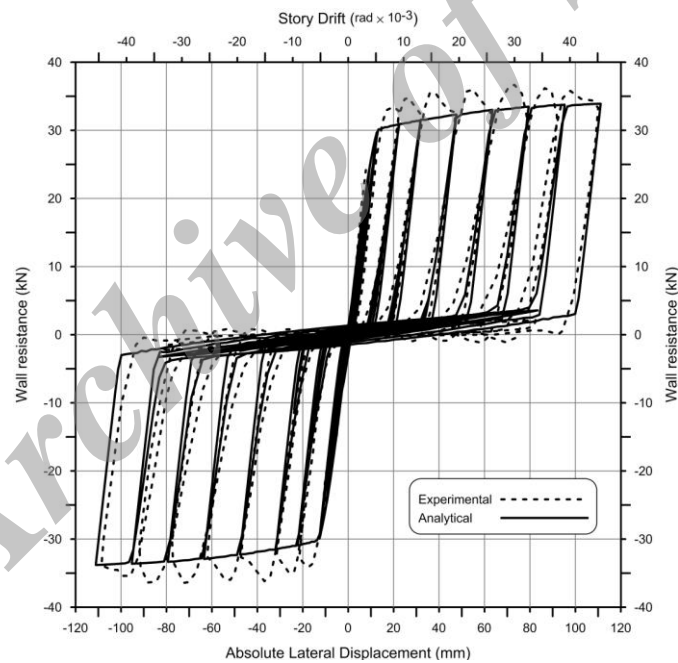
Figure 4. Deformed shape of the FE model after 110 s



Figure 5. Hysteresis cycles obtained from experimental specimen and the FE model

Table 2: Comparison of FE results with the experimental data

| ID: 14 A-C | $k$ (kN/mm) | | | $P_u$ (kN) | | |
|---|---|---|---|---|---|---|
| | Experiment | FE | Error (%) | Experiment | FE | Error (%) |
| Negative | 2.80 | 2.885 | 3.04 | 36.59 | 33.80 | 7.63 |
| Positive | 2.93 | 2.903 | 0.91 | 36.72 | 33.91 | 7.65 |

## 3. RESULTS AND DISCUSSION

In this section, results of FE analysis of the investigated model, including hysteresis behavior, internal forces, and failure mechanism, are discussed.
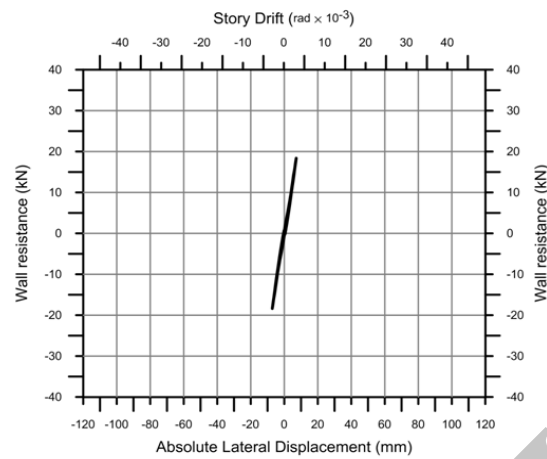
### 3.1 Hysteresis curves

There are three types of hysteresis loop based on applied displacement amplitude for the analyzed cold-formed frame. The first type observed for the first 62.12 s is shown in Fig. 6a. Shapes of these loops indicate the elastic behavior of frame within the time of investigation. Lower residual strains, partial yielding in braces at the connection region with chord studs, and track buckling initiation were observed during the FE analysis.

The second type of hysteresis loop was seen from 62.12 s to the end of the loading (102 s) as shown in Fig. 6b. In this type of loops, the yielding of tensile braces occurred at 0.0054 rad. When tensile and compressive braces were yielded and buckled, the displacement applied in the reverse direction led to the loosing of braces' load carrying capacity until point "a". Furthermore, at this point, tensile and compressive braces were converted respectively to compressive and tensile braces. The stiffness of frame at point "a" suddenly reached about 80% of initial stiffness value with increasing the value of applied displacement. At this point, the tensile brace obtained its load carrying capacity again.
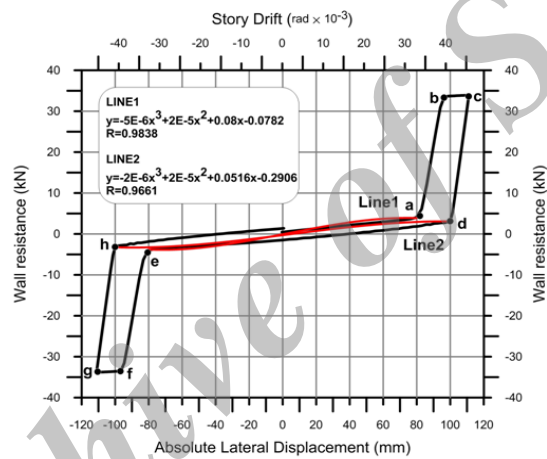
More loading caused the tensile brace to yield at point "b" and frame lateral stiffness was decreased to 1.5% of the initial stiffness. This stiffness is due to the presence of hold-downs and rigid connection of tracks and studs. Unloading was begun at point "c". First unloading line slope was greater than the initial stiffness until point "d" and after that, unloading continued with 1.5% of the initial stiffness until point "e". All of above steps were repeated in negative loading. The tensile brace strain was reached the maximum generated residual strain in previous loop at points "a" and "e" which were initial points of tensile braces loading. The tensile brace obtained its load carrying capacity for current loop at these points. Points "d" and "h" were the unloading points of tensile braces. The variation of principal logarithmic strain versus time of experiment is presented in Fig. 7 for a point located on the brace at the middle of two screw connections. In this figure, the points "a" to "h" show the status of investigated frame corresponding to points "a" to "h" in Fig. 6b. Line 1 represents the maximum applied strain for studied brace in the previous loop which is equal to the initial strain value for the next loop and Line 2 shows the initial strain for the latter loop. The small vertical distance between "a" and "c" indicates tensile residual yielding strain. Negative loading and buckling of brace had major contribution to the increase of residual strain and caused the residual strain axis to shift to point "g".

Based on the results of FE analysis, it can be said that considerable energy dissipation in cold-formed frame was occurred in the second type of loops. In this case, braces behave as efficient energy damping elements via their buckling and yielding. The severe buckling of braces and local buckling of tracks are the main characteristics of these loops. Hold-downs experienced minor yielding until the end of the loading indicating the suitable size of these members. Measured values of stiffness for different portions of this loop are given in Table 3.
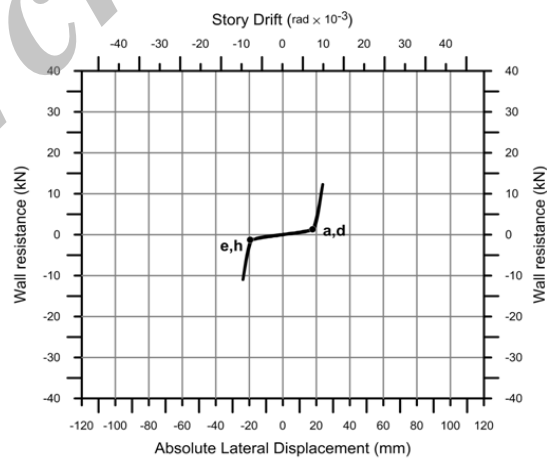
If the displacement applied to the structure was lower than the maximum applied displacement in previous loop, the yielding points "b-c" and "g-f" would not be formed and loading and unloading points of braces would coincide as shown in Fig. 6c.

Figure 6. Various hysteresis cycles observed during the loading of the model: (a) elastic region, (b) inelastic region, (c) inelastic region with small amplitude
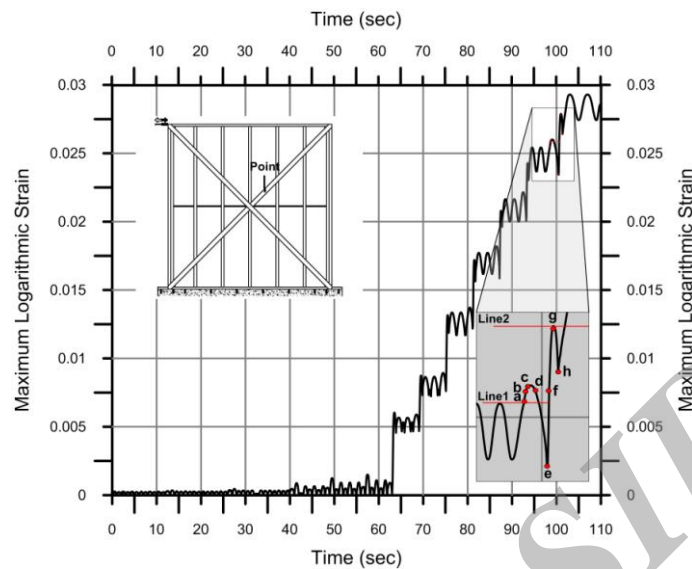
Figure 7. Maximum logarithmic strain at the midpoint between two inner columns

Table 3: Lateral stiffness of the structure in the inelastic region during various stages of loading

| Label | Stiffness | Stiffness coefficient ($\alpha$) | | | Description |
|-------|-----------|------|------|------|-------------|
|       |           | Min. | Max. | Avg. |             |
| a-b   | $\alpha_1\ k^+$ | 0.8 | 0.85 | 0.82 | Positive loading stiffness |
| b-c   | $\alpha_2\ k^+$ | 0.006 | 0.03 | 0.015 | Stiffness of plasticity region due to positive loading |
| c-d   | $\alpha_3\ k^+$ | 1.02 | 1.03 | 1.023 | Positive unloading stiffness |
| d-e, h- | $\alpha_4\ k^+$ | 0 | 0.02 | 0.015 | Transmission region stiffness |
| e-f   | $\alpha_5\ k^-$ | 0.75 | 0.82 | 0.8 | Negative reloading stiffness |
| f-g   | $\alpha_6\ k^-$ | 0.006 | 0.023 | 0.015 | Stiffness of plasticity region due to negative loading |
| g-h   | $\alpha_7\ k^-$ | 1.016 | 1.033 | 1.026 | Negative unloading stiffness |

*3.2 Bolt's force*

The variation of shear and axial forces of screws and corresponding envelopes are presented in Fig. 8. It can be seen in this figure that the screws' maximum shear and axial pull-out forces had been 1.06 kN and 1.15 kN, respectively; which were less than their ultimate strength. The maximum shear and axial force were generated at the top and middle screws. Two remarkable observations were made: (1) Maximum shearing force of screws was generated at 62.12 s; and (2) According to Fig. 8a, considerable decrease in shearing force occurred at 63.13 s. The first one is due to brace yielding and the second one is due to the inversion of loading direction. Therefore, the shearing force of screws will reduce with brace yielding. The evaluation of screws' axial force variation showed two turning points at 62.12 s and 80 s. The increase of axial force was considerably decreased at 62.12 s and the

maximum axial force was generated at 80 s as shown in Fig. 8b. After this moment, the value of axial force remained almost constant with the increase of loading amplitude (Fig. 8a). The maximum shearing and axial forces of screws were generated at tensile brace and buckled brace, respectively. The stability of axial force was due to the development of local yielding in buckled brace at the 80th second of loading.
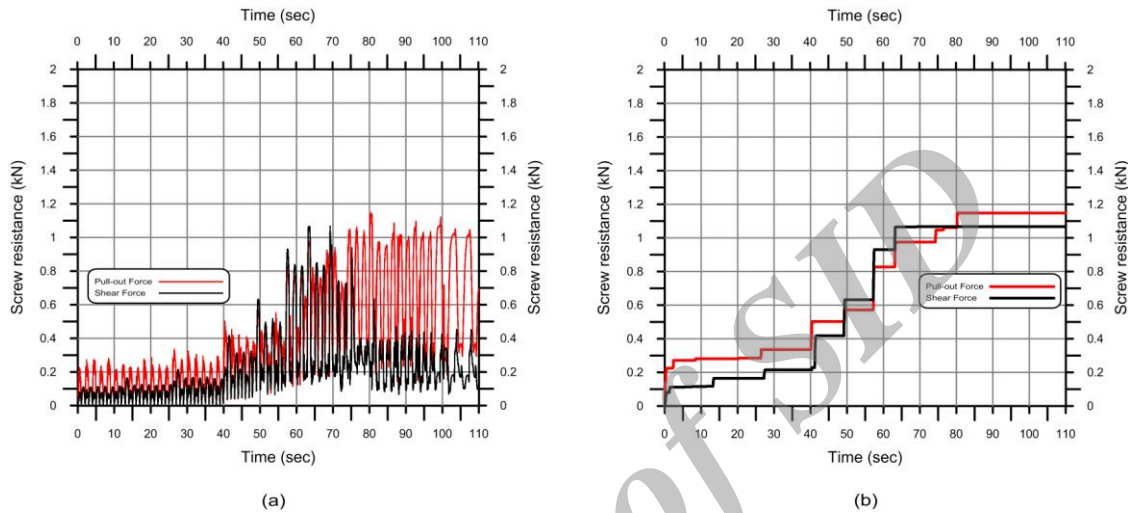
Figure 8. Temporal variation of (a) shear and axial forces of screws, and (b) corresponding envelopes

## 4. CONCLUSIONS

In the present research, a FE model was developed to investigate the cyclic behavior of cold-formed steel frames. Two dimensional S4R shell elements with reduced integration were used. A method for simulating the real behavior of screws was presented. Shear and axial pull-out failures were simulated by radial-thrust connector element for self drilling screws. Frictional contact between braces and studs along with material and geometrical nonlinearities were considered. The accuracy of FE results was verified using experimental data. The main findings can be summarized as follows.

Lateral stiffness of the studied frame at the elastic region for positive loading was calculated as 2.9 KN/mm which was a little bit different from the result of negative loading. By entering the inelastic region at 62.12 s, the amount of stiffness was reduced to 80% of elastic region's value on an average sense. The study of recorded cycles indicated the structure's efficient energy dissipation at the inelastic region of braces via their buckling and yielding. According to the conducted studies, the effect of braces' buckling on the creation of residual strain and energy dissipation is more than the effect of these members' yielding due to the tension.

By studying the generated forces in connector element which simulates the screw's behavior, the maximum value of screw's shear and axial forces were determined as 1.06 kN at the top screw and 1.15 kN at the middle screw, respectively. These values were lower than the

ultimate strength of screws and therefore no failure was observed at the FE model. Studying the screw's shear force diagram indicated that the maximum shear force occurs at the moment the frame enters the inelastic region (62.12 s). After this moment, with braces yielding, not only there would be no increase in the amount of this force but also a rather perceptible reduction would be developed. Entering into the inelastic region, at first, caused a falling in the rate of increase of the screw's axial force and then led to the occurrence of severe buckling. The axial force reached its maximum value at 80 s and then stayed constant.

In cold-formed frames with cross strap braces, entering into inelastic region is very important because it leads to efficient energy dissipation. It is crucial that the columns and connection tools do not buckle or fail prior to this stage. The present paper, in addition to presenting a method for FE modeling of frames with cold-formed members and cross braces, investigated the behavior of frame and its connections under cyclic loading. Results can provide a better insight into the efficiency of cold-formed frames with cross strap braces especially regarding their energy dissipation characteristics.

# REFERENCES

1. American Iron and Steel Institute (AISI), North American standard for cold-formed steel framing-lateral design−S213, Washington DC, US, 2012.
2. American Iron and Steel Institute (AISI). Inelastic performance of welded CFS strap braced walls, Research Report, Department of Civil Engineering & Applied Mechanics, McGill University, Montreal, Canada, 2008.
3. Adham SA, Avanessian V, Hart GC, Anderson RW, Elmlinger J, Gregory J. Shear wall resistance of lightgage steel stud wall systems, *Earthquake Spectra*, No. 1, **6**(1990) 1-14.
4. Al-Kharat M, Rogers CA. Inelastic performance of screw connected cold- formed steel strap braced walls, *Canadian Journal of Civil Engineering*, No. 1, **35**(2008) 11-26.
5. Al-Kharat M, Rogers CA. Inelastic performance of cold-formed steel strap braced walls, *Journal of Constructional Steel Research*, No. 4, **63**(2007) 460-74.
6. Kim TW, Wilcoski J, Foutch DA, Lee MS. Shake table tests of cold-formed steel shear panel, *Engineering Structures*, **28**(2006) 1462-70.
7. Filiatrault A, Tremblay R. Design of tension-only concentrically braced steel frames for seismic induced impact loading, *Engineering Structures*, No. 12, **20**(1998) 1087-96.
8. Hatami S, Ronagh HR, Azhari M. Behaviour of thin strap-braced cold-formed steel frames under cyclic loads, *Proceedings of The 5th International Conference on Thin-Walled Structures*, Brisbane, Australia, **1**(2008) pp. 363-370.
9. Husem M, Pul S, Yozgat E, Gorkem SE. Fracture of the connections between steel and reinforced concrete shear walls under the cyclic loading, *Iranian Journal of Science and Technology, Transactions of Civil and Environmental Engineering*, No. C1, **36**(2011) 97-102.
10. Dalalbashi Esfahani A, Mostofinejad D, Mahini S, Ronagh HR. Numerical investigation on the behavior of FRP-retrofitted RC exterior beam-column joints under cyclic loads, *Iranian Journal of Science and Technology, Transactions of Civil and Environmental Engineering*, No. C1, **35**(2011) 35-50.

11. Sharbatdar MK, Dalvand A, Hamze-Nejad A. Experimental and numerical assessment of FRP stirrups distance on cyclic behavior of RC joints, *Iranian Journal of Science and Technology, Transactions of Civil and Environmental Engineering*, No. C$^+$, **37**(2013) 367-81.
12. Sorensen Inc, ABAQUS user's manual, US, 2010.
13. American Iron and Steel Institute (AISI), Supplement No. 2 to the North American specification for the design of cold-formed steel structural members–S100, Washington DC, US, 2012.